DELFT UNIVERSITY OF TECHNOLOGY
Faculty of Civil Engineering and Geosciences

Report

SECTION OF APPLIED GEOPHYSICS AND PETROPHYSICS

Report on ground-penetrating radar techniques for seawall asphalt pavement investigations

Dr.ir. E.C. Slob
Department Geotechnology
Mijnbouwstraat 120 • room 217
2628 RX Delft, The Netherlands
Phone 3115 2788732 • Fax 3115 2781189
Email E.C.Slob@TuDelft.nl

Table of Contents

Report:
Ground-penetrating radar techniques for asphalt pavement investigations, with emphasis on seawall pavements

Dr.ir. E.C. Slob
Applied Geophysics and Petrophysics
Department Geotechnology
Delft University of Technology

This report discusses possibilities of using radar technology in asphalt pavement investigations in several types of pavement. The main focus is on highly porous asphalt (OSA) and watertight asphalt concrete (WAB), as used in Dutch seawalls. The determinations of layer thickness as well as layer integrity are important goals. The asphalt pavements as discussed are used on seawalls and therefore saline environments receive special attention as they affect the penetration depth most. References given come from the public domain, no attempt has been made to access private domain publications. Several internet addresses of companies in the private domain are listed at the end.

1 Basic information

Radar technologies rely on the propagation and reflection of electromagnetic waves in the medium to be probed. Hence applications where sufficient contrasts in electromagnetic wave velocities occur are worth investigating. Here the investigation is carried out in the context of asphalt pavement thickness and integrity.

Since the nineteen seventies, ground-penetrating radar techniques have been investigated in many countries in the world for road deck inspection. Initially GPR was used in tunnel applications, later investigations in detection of subsurface distress in bridge decks were added and in the mid-eighties van-mounted GPR's were established for national highway inspections. Since the nineties it has become a large commercial application and several specialized companies exist around the world. Internet addresses of several specialized companies and GPR manufacturers are given at the end of the references list.

1.1 Detection and localization of changes

GPR as a profiling tool can operate as a detector of the changes in fluid-filled porous zones. These zones occur as a sudden change in electromagnetic wave velocity because the velocity in water is nine times smaller than in water free zones. Of course, in a closed asphalt concrete these zones occur because of wearing or cracking in combination with imperfections in the surface sealing capacity or because of upward infiltration of subsurface water. In this mode of operation also changes in different layer thicknesses can be detected as well as changes in the surface due to stripping or other causes, which method is expected to be extremely effective in time-lapse monitoring. In Chapter 3 we show an example of the expected effective electric permittivity value as a function of void porosity and water saturation and we use these values in an example of expected GPR reflection data of a bituminous asphalt layer sequence to illustrate the expected effect of a degraded layer.

For ground-coupled GPR antennas careful calibration is needed to make an estimate of the propagation velocity in the layers in case single channel GPR systems are used. Modern multi-channel systems allow the simultaneous measurement with several, spatially displaced, receiving antennas for each transmitter antenna position. The analysis of this type of data allows for continuous propagation velocity estimates as a function of depth. The accuracy of these estimates increases with the number of receiving antennas and horizontal offset range. The advantages of such methods are real-time automated layer thickness estimates and increased accuracy of the estimates. Even though multi-offset measurement and their use in velocity analysis are very well known and suitable for thickness estimates, there are not many accounts of it for pavement investigations (Hugenschmidt, 2000). An additional advantage could be the real-time detection of degraded zones, but this is still subject to research.

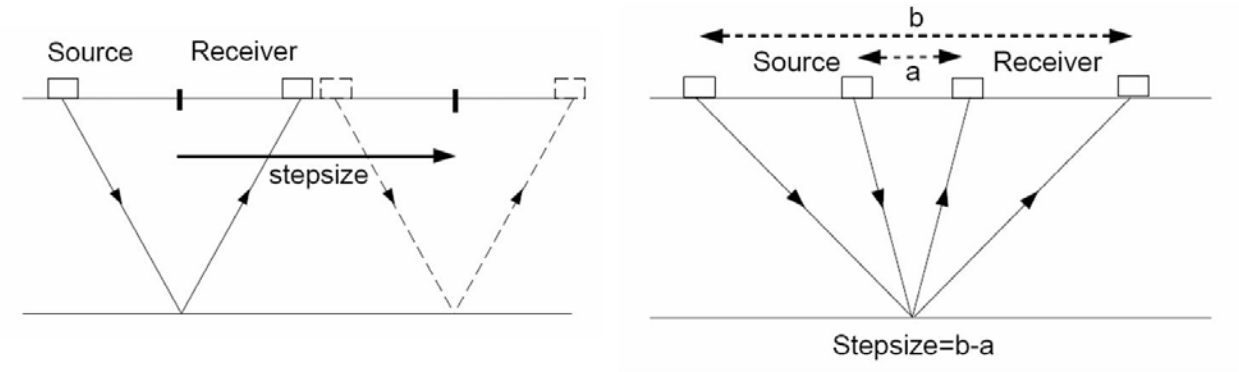

Figure 1. Schematic drawing of a common-offset, or fixed-offset, measurement, usually employed in GPR profiling (left) and a common-mid-point (CMP) measurement, usually employed for vertical velocity profile determination (right).

To detect changes in a recorded profile as a function of antenna position does not give a decisive answer to the question of determining asphalt layer thickness, degradation, changes in porosity or in the fluids filling the pore space. The radar is sensitive to electromagnetic changes in the subsurface. To translate these to an answer to the questions requires a so-called constitutive model that predicts how the electromagnetic properties will change if a certain change in layer thickness, layer integrity, porosity or filling fluid would occur. Many constitutive models exist and most are purely based on experimental history matching. Some accounts of this work are Al-Qadi *et al.* (2000), Liu and Guo (2002), Millard *et al.* (2002), Benedetto (2004) and Adous *et al.* (2006), who performed theoretical or experimental investigations in characterization of pavement material under various conditions. An overall conclusion is that different materials used in pavements behave differently and that no theoretical model is presently available that can account for known experimental GPR results on pavements. The spatial variability of the pore space in volumes smaller than the wavelengths used, in combination with different filling fluids, plays an unknown role. It is not only the total volume fractions that constitute the whole mixture that determine the bulk properties, but also their volumetric distribution at scales smaller than the wavelengths of operation. Results on gravel roads are also reported (Saarenketo and Vesa, 2000). Sometimes different asphalt layers can be detected because their electromagnetic properties differ sufficiently from each other to give rise to a measurable reflection. Damage inside asphalt layers are explicitly treated in Lorenzo et al. (2000) and Benedetto *et al.* (2004) and Benedetto and Pensa (2006). Lorenzo found degradation because of increased porosity values indicated loss of structure integrity in the concrete floors, while Benedetto et al. (2004) and Grote et al. (2005) evaluated the effectiveness of water infiltration on the pavement surface in order to use GPR in pavement damage detection. Finally, a different low frequency method is described by Dashevsky *et al.* (2005) who designed and constructed a capacitive apparatus to measure layer thickness and integrity.

Many publications on thickness evaluations and road inspection, for sub-base grade up to surface asphalt layer quality determination, exist, mostly in conference proceedings. Some important examples are Roddis et al. (1992), Hugenschimdt (1998), Fernando et al. (2000), Slob et al. (2001), Jung et al. (2004) and Kao et al. (2006). All these report highly successful results in layer thickness evaluations, effects of soft soil to settlement and different layer permittivity estimates, on very different types of asphalt pavements also the sub-grades and the soil below the total pack have been evaluated in some of these studies. Modern equipment is capable of performing measurements at highway speeds (100 km/h) so that there is no necessity for lane closure or protection. The work of Slob in 1998 (published in 2001) has lead to a sufficient confidence level in the Netherlands to perform GPR inspections for road decks at the network level. Unlike many countries in Europe, the United States of America and Canada, in the Netherlands GPR inspection is not implemented as a routine operation. The works described above use bi-static fixed-offset GPR data and either CMP measurements at several locations, see Figure 1, or core drillings for calibration and rely on the absence of strong lateral changes in electromagnetic properties for layer thickness determination. A different approach to thickness evaluation is by using mono-static off-ground GPR, where the transmitting antenna is the same as the receiving antenna. This set-up can be calibrated to a high degree of accuracy and a multi-layered medium can be used as a model for the asphalt layers and the medium below it. One of the earliest accounts on this approach that is dedicated to asphalt pavement thickness determination is Spagnolini (1997) and which method has been improved by Lambot *et al.* (2004) for hydrogeophysical applications. The advantage of this method is that for every measurement position a new depth profile of

permittivity is computed without the need for calibration with core drillings and without the assumption of laterally smooth changes in material properties.

1.2 Different systems and acquisition set ups

In the previous paragraph, several different GPR techniques have been mentioned that are described in more detail here. Radar systems exist as air-launched antenna systems and ground-coupled antenna systems, as shown in Figure 2. The advantage of air launched antennas is the fact that antenna and medium to be probed are decoupled if the antenna height is sufficiently large. Then the antenna behaviour is independent of the medium and can be characterized and calibrated for by a set of independent measurements. This applies to both time-domain or pulse radars and frequency domain (continuous or stepped) radars. The main advantage of ground-coupled systems is the maximum energy that is sent into the ground in combination with a wide radiation pattern. Time domain radars acquire data through subsampling, where for each transmitter excitation a single time sample is recorded. This explains why pulse GPR is a relatively slow measurement. The use of existing modern electronics components in commercial GPR systems will allow for real time sampling, which will speed up the pulse radar recordings tremendously. Frequency domain radars sample a single frequency for each transmitter excitation and usually apply time gating to reduce signal return ambiguity. Here a similar problem with acquisition speed exists, which will be reduced when real time sampling becomes commercially available and the whole frequency band can be swept in (near) real time.

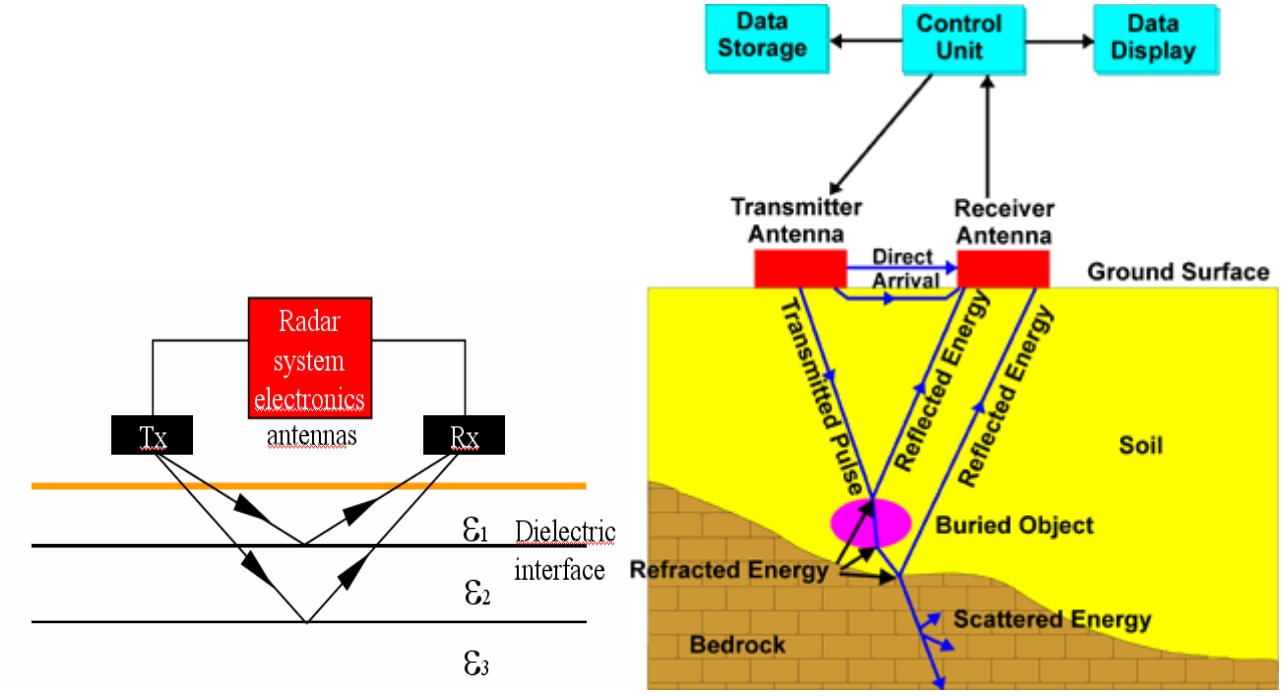

Figure 1. Examples of air-launched antennas (left) and ground-coupled antennas (right) used in different GPR systems.

System performance is usually given in terms of parameters for which a specific GPR is optimized (Mesher *et al.*, 1995, Manacorda and Miriati, 2000, Fauchard *et al.*, 2000 and 2003, Hugenschmidt, 2004, and Grivas and Shin, 2004). These are

1. System dynamic range, defined as $DR_{sys} = 20^{10}\log(\max(amp)/\min(amp))$, but the sampling dynamic range is what determines the actual measurable signal range (which is 96 dB for a 16 bit recording system);

2. Frequency bandwidth or its inverse Pulse width. One can always define the bandwidth as the 3 dB bandwidth in frequency domain (the difference between maximum and minimum frequency where the signal is less than 3 dB less than the maximum amplitude). Bandwidth determines the resolution in the direction away from the antenna also known as range resolution;

3. Pulse repetition frequency, which determines how fast two consecutive measurements can be taken and depends on the recovery time of the electronic components and the antennas used;

4. Unambiguous range (for frequency domain radars), which is defined as the maximum distance from the antennas that is uniquely defined and is related to Nyquist's sampling criterion for time domain systems.

Lateral, or cross-range, resolution is not a design specification because it is determined by the range of a target and the propagating velocities of the electromagnetic waves. Signal processing techniques like imaging are used to improve lateral resolution.

Antenna position information is the most important factor of success in a GPR investigation. Position information is indispensable for focusing of reflection and scattering events back to their location of origin and allows one to find target spots after data collection and processing. This is true in any investigation where the data is taken to the laboratory for further processing and interpretation, but especially for high speed investigations like on highways and railroads, where huge amounts of data are collected, knowledge of antenna position for each measurement is an important factor.

Finally one can choose between different antennas (Kong, 2000) for transmitting and receiving the signals. Since the transmitter is excited, it has a high amplitude signal going through. When the same antenna is used as a receiving antenna, this signal has to be recorded without saturating the receiver bits otherwise one looses information from the shallow part of the subsurface whose return arrives back into the transmitter antenna before the transmitted signal has left the antenna. Taking into account that the return signal is roughly 1000 times smaller than the transmitted signal, a fixed sampling dynamic range limits the properly recorded return signal. This problem is overcome by using a second and separate antenna to record the return signal. Then the whole sampling dynamic range can be used to record only return signals and usually the strongest signal is the signal that corresponds to the direct coupling between the transmitter and receiver (direct arrival either through the air or through the ground). High accuracy calibration of a two-antenna recording system is more difficult than of a single antenna system (Olhoeft and Smith, 2000, Huang and Su, 2004, Lambot *et al.*, 2004).

2 Accuracies and resolutions

To decide if acquisition of GPR data is sensible or not in the above-mentioned applications, it is necessary to get some idea of the possible accuracies and resolutions that can be expected from such surveys.

2.1 Propagation, dispersion and medium parameters

We are normally tending toward saying that radar data can only be acquired in frequency bands where the propagating part of the total electromagnetic field dominates. In marine environments, with an inherent high-conductivity of sea water, this might not be a workable situation so we investigate here also the effect of high salinity water inside the pore space of asphalt concrete on the signal that enters this asphalt layer to see if the reflection return from the bottom of the asphalt layer has a high enough amplitude to be recorded. We first give some rule of thumb formulas and numbers for electric impedance, wavelength and the related penetration depth and resolution.

The propagation velocity in free space is defined as $c_0 = 2997921458$ m/s. We consider all materials to be non-magnetic; hence, they are all characterized by the magnetic permeability of free space, $\mu_0 = 4\pi \times 10^{-7}$ H/m. This is a reasonable assumption and in cases where it is not, still the error involved with the assumption is small. Two quantities are important in assessing the applicability of GPR. These are electric impedance and the propagation factor. The difference in electric impedance between two adjacent media determines the reflection strength of the transition. Impedance is usually given in terms of the plane wave impedance as

$$Z = \left(\frac{\mu_0}{\varepsilon - \mathrm{i}\sigma/\omega} \right)^{1/2} = Z_0 \left(\varepsilon_r - \mathrm{i}\,\sigma/\omega\varepsilon_0 \right)^{-1/2}; \omega = 2\pi f , \quad (1)$$

where Z_0 is the free space impedance in Ω, conductivity is denoted σ in 1/(Ωm), $\varepsilon=\varepsilon_0\varepsilon_r$ is the electric permittivity and is the product of the free space permittivity, $\varepsilon_0 = 1/(\mu_0 c_0^2)$, and the relative permittivity, ε_r, while ω is radial frequency. Generally speaking all these parameters are depending on the frequency value, but for most materials encountered in the earth and for bituminous asphalt concretes it is reasonable to assume that this dependency is smooth over the frequency bands used in GPR applications. In a homogeneous medium, the electric conductivity and permittivity are constants. Then the spherical wave propagation factor is given by

$$\gamma = \sqrt{i\omega\sigma\mu - \omega^2\varepsilon\mu} = \gamma_r + i\gamma_i, \quad \gamma_r = \frac{\omega}{c}\left(\frac{1}{2}\sqrt{1+\left(\frac{\sigma}{\omega\varepsilon}\right)^2} - \frac{1}{2}\right)^{1/2} \text{ and } \gamma_i = \frac{\omega}{c}\left(\frac{1}{2}\sqrt{1+\left(\frac{\sigma}{\omega\varepsilon}\right)^2} + \frac{1}{2}\right)^{1/2}, \quad (2)$$

Where $c = c_0/\sqrt{\varepsilon_r}$ is the velocity with which an electromagnetic wave propagates and it is observed that if the conductivity σ=0, the real part of γ is also 0. From these two observations it can be concluded that the *real* part of γ represents the *attenuation* part, while the *imaginary* part of γ represents the *propagating* part. For conductive media the propagation factor is complex and only for very small values of the conductivity relative to the product of frequency and the permittivity, the imaginary part is equal to the phase wave number and the real part is a constant given by

$$\gamma_r = \frac{\sigma}{2}\sqrt{\frac{\mu}{\varepsilon}} \quad \text{and} \quad \gamma_i = \frac{\omega}{c} = \frac{2\pi}{\lambda}, \quad (3)$$

where λ denotes the wavelength in m. Equation (3) is known as the *high-frequency* limit. The *attenuation* is described by γ_r and the wave *propagation* by γ_i. In general, the complex square root must be taken as indicated in equation (2). The propagation is determined by taking the exponential of the complex propagation factor. Then the two-way amplitude decay per meter is given in decibels by

$$AD = 10\log_{10}\left(\exp\left[-2\gamma_r\right]\right) = -8.686\gamma_r. \quad (4)$$

In addition to amplitude loss, due to irreversible energy conversion from electromagnetic wave energy into heat, also the phase velocity is frequency dependent. This leads to shape distortion of the wavelet transmitted by the source antenna into the homogeneous embedding. This distortion leads to an error in the estimated phase if this not taken into account and the phase error amounts to

$$\varphi_{err} = 1 - \left(\frac{1}{2}\sqrt{1+\left(\frac{\sigma}{\omega\varepsilon}\right)^2} + \frac{1}{2}\right)^{1/2} \quad (5)$$

The phase error is defined as unity minus the ratio of the actual phase wave number (eq. (2)) and the high-frequency limit of the phase wave number (eq. (3)).

In the examples below we use effective electric parameters of the bulk consisting of solid components (bitumen, stones, sand) and fluid components (air, water), while the mixture rule employed is discussed in Section 2.3. Some results for the attenuation in decibels per meter defined in equation (2) and phase errors defined in equation (5) and we use the exact formulas to show how much they differ from the high-frequency approximation. Results are shown Figures 3a to 3d, for two different permittivity values that can be encountered in asphalt layers and soil. The right column, plots a) and b), show the results for water free asphalt with a relative permittivity of ε_r=5, while the left column, plots c) and d) show results for a water saturated 45% porosity asphalt with a relative permittivity value of ε_r=20 (see Section 2.3). The attenuation is shown as a function of frequency and conductivity in a) and c), while the phase distortion is shown as a function of frequency and conductivity in b) and d). As can be seen from

the formulas in equations (2)-(5) the effects of conductivity become constant with increasing frequency, for which reason the maximum frequency chosen here is 500 MHz.

Similar results are shown in Figure 4a to 4d, as a function of frequency and relative permittivity for two different fixed conductivity values of σ=0.05 S/m in a) and b), and for σ=0.1 S/m in c) and d). It is observed that if we accept an attenuation of 20 dB in two-way propagation for 1 meter of penetration (hence the two-way travel distance is 2 m), the maximum allowable conductivity is σ=0.03 S/m for a relative permittivity of ε_r=5, while it is σ=0.06 S/m for a relative permittivity of ε_r=20. This is because attenuation scales as conductivity divided by the square root of relative permittivity. This is reasonably correct for the frequencies considered from 100 MHz to 500 MHz. The phase distortion is within the 10% range for those conductivities over the considered frequency bandwidth.

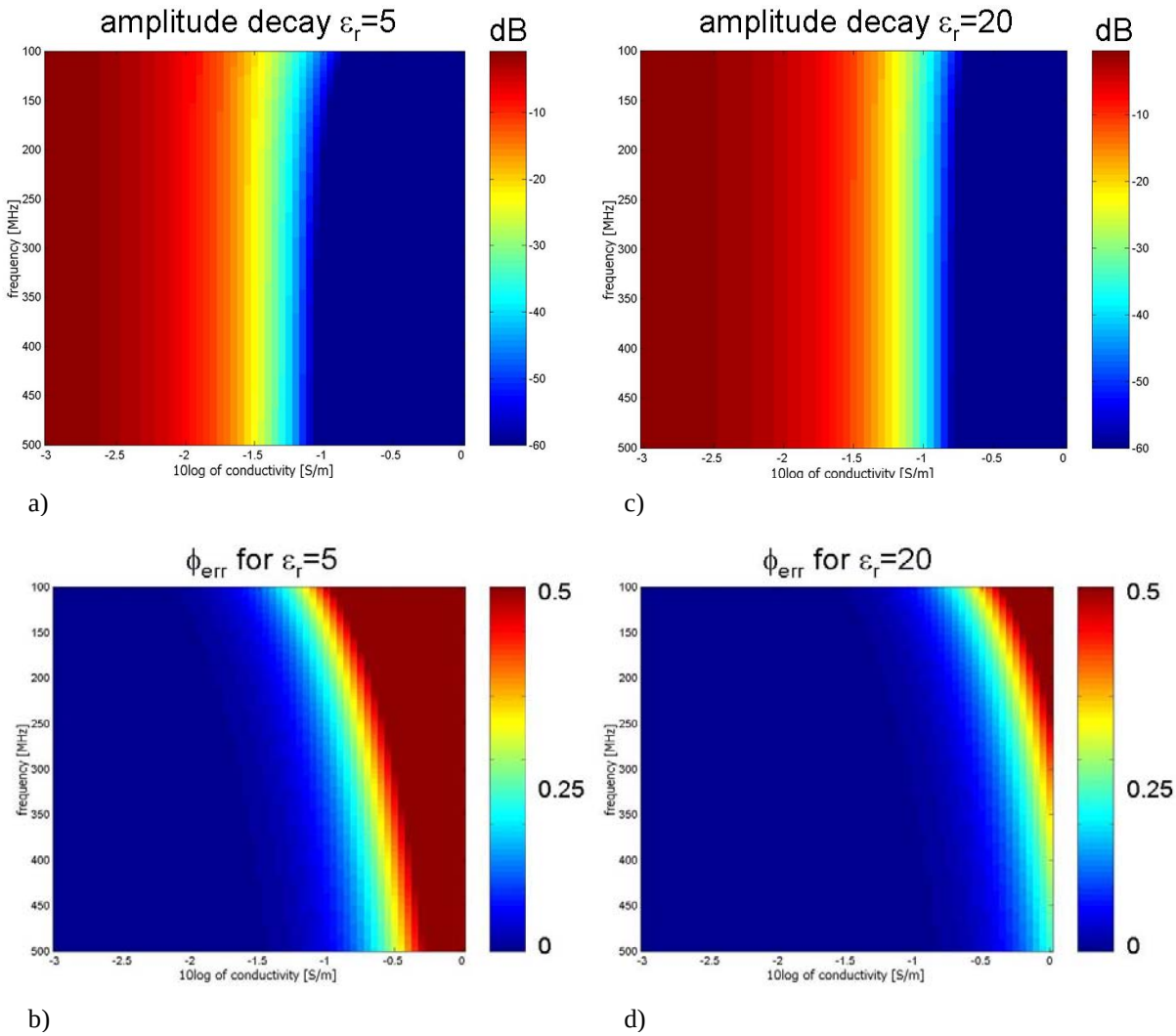

Figure 3: Two-way attenuation and phase distortion per meter penetration for two fixed relative electric permittivity values, as a function of frequency and conductivity.

For the conductivity value of σ=0.05 S/m, or a resistivity of 20 Ωm, a relative permittivity of minimally ε_r=16 is required, which number increases to ε_r=20 for a resistivity of 10 Ωm. In the latter case, only frequencies higher than 200 MHz can be used. For all these cases, the frequency distortion is negligible.

The 30 dB attenuation level for propagation loss is reasonable as a threshold value because also energy will be lost in the propagation due to geometrical spreading (around 3 to 6 dB) and due to the reflection and transmission process (depending on the contrast, up to 10 dB). The total amplitude loss is then roughly 45 dB and this can be accurately recorded by modern data acquisition systems.

For higher frequencies than the ones used here the situation is more favourable because attenuation due to conductivity per meter becomes a constant and phase distortion can be neglected. From this we conclude that shallow investigations, with a target penetration depth of less than 1 m and with high-frequency GPR equipment (with a bandwidth ranging from 500 MHz to 3 GHz) should be feasible with a high degree of accuracy in thickness determination and damage detection if damage can be associated with increased water or brine in the asphalt pore space. The actual success will depend on the size of the stones with which the asphalt layers are constructed and the amount of water in the formation. This is because with increasing water content the effective wavelength becomes smaller and for fixed size grains in the asphalt electrically speaking the grains become larger, leading to increased clutter levels.

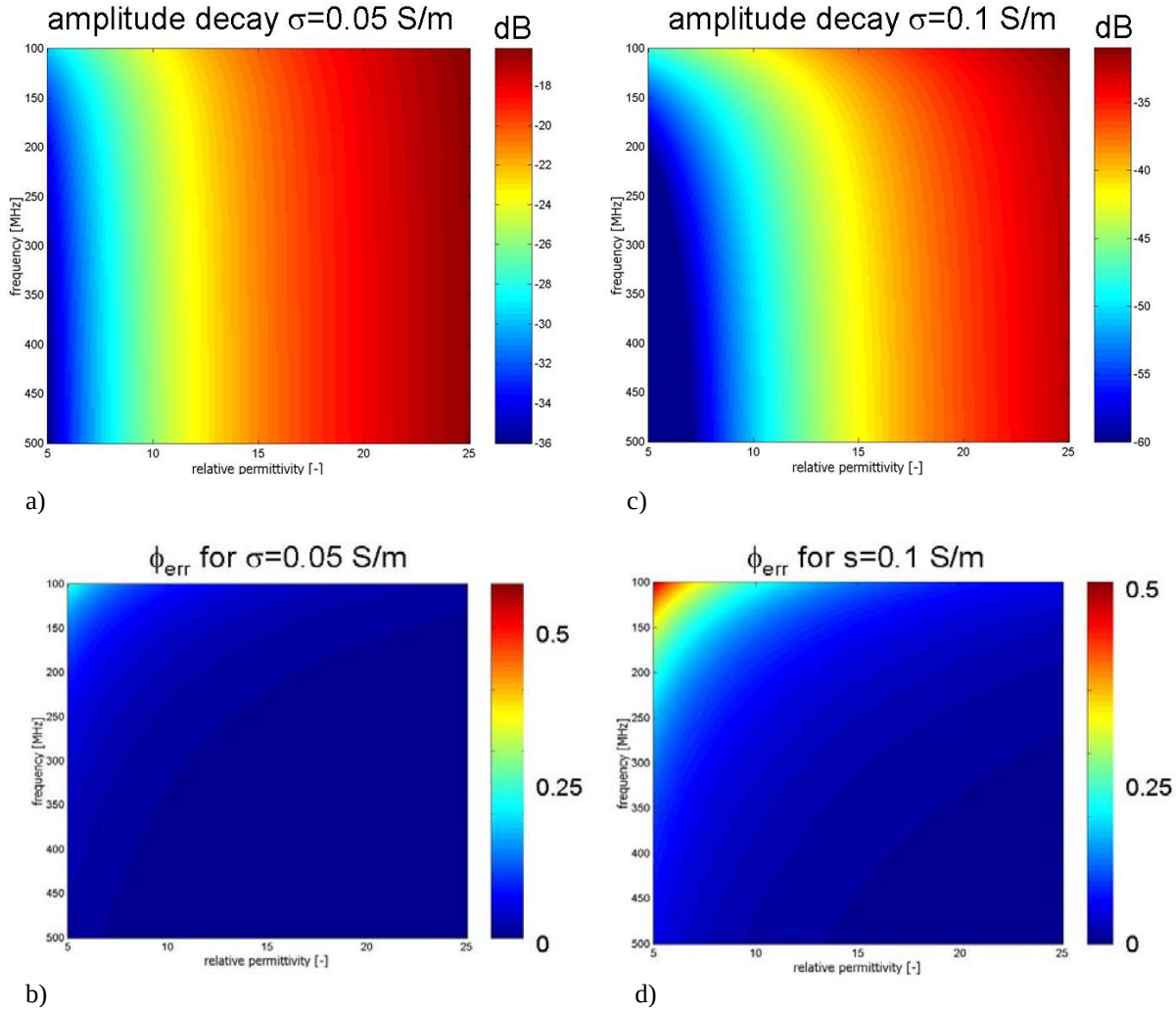

Figure 4: Two-way attenuation and phase distortion per meter penetration for two fixed electric conductivity values, as a function of frequency and relative electric permittivity.

2.2 Reflection & transmission

The amount of electric contrast determines whether ground penetrating radar is feasible or not. Depending on the situation, this is primarily determined by the electric permittivity and/or the electric conductivity, as the magnetic permeability is nearly constant and equal to the free space value. Here two different situations are investigated, a planar interface with a contrast in electric conductivity and permittivity.

$$r^{TE} = \frac{\sqrt{\left[\cos(\theta)\right]^2 - i\frac{\sigma_1}{\omega\varepsilon_1}} - \frac{c_1}{c_2}\sqrt{1 - \frac{c_2^2}{c_1^2}\left[\sin(\theta)\right]^2 - i\frac{\sigma_2}{\omega\varepsilon_2}}}{\sqrt{\left[\cos(\theta)\right]^2 - i\frac{\sigma_1}{\omega\varepsilon_1}} + \frac{c_1}{c_2}\sqrt{1 - \frac{c_2^2}{c_1^2}\left[\sin(\theta)\right]^2 - i\frac{\sigma_2}{\omega\varepsilon_2}}}, \quad (6)$$

and

$$r^{TM} = \frac{\sqrt{\left[\cos(\theta)\right]^2 - i\frac{\sigma_1}{\omega\varepsilon_1}} - \frac{\eta_1 c_1}{\eta_2 c_2}\sqrt{1 - \frac{c_2^2}{c_1^2}\left[\sin(\theta)\right]^2 - i\frac{\sigma_2}{\omega\varepsilon_2}}}{\sqrt{\left[\cos(\theta)\right]^2 - i\frac{\sigma_1}{\omega\varepsilon_1}} + \frac{\eta_1 c_1}{\eta_2 c_2}\sqrt{1 - \frac{c_2^2}{c_1^2}\left[\sin(\theta)\right]^2 - i\frac{\sigma_2}{\omega\varepsilon_2}}}, \quad (7)$$

where θ denotes the angle of incidence and the parameter $\eta_i=\sigma_i+i\omega\varepsilon_i$. These formulas are exact as far as plane waves incident on a flat interface are concerned, where the angle of incidence is relative to the normal vector of the interface. The TE-mode reflection coefficient contains the velocity ratio in the second terms in the numerator and denominator, while the TM-mode reflection coefficient contains the admittance ratio in the second terms in the numerator and denominator. The TE-mode reflection coefficient corresponds to waves whose electric field vector is perpendicular to the plane spanned by the propagation direction and the depth axis, while the TM-mode reflection coefficient corresponds to waves whose electric field vector points in that plane.

For the same values as used for Figures 3 and 4, here the results are shown for the reflection amplitudes in Figure 5. We use the low permittivity and conductivity values for the medium where the incident wave travels (intact surface layer) and the higher permittiivty and conductivity values for the medium behind the reflector (degraded lower layer). We take for the first medium, σ=0.05 S/m, or a resistivity of 20 Ωm which seems a high conductivity value, but it is probably a realistic value given in-situ temperature and salinity conditions in the extreme environment of sea dikes.

We take a relative electric permittivity of $\varepsilon_{r;1}$=5, while the relative electric permittivity in the second medium varies from 5 to 25 in Figure 5a for the TE-mode and in Figure 5c for the TM-mode reflection. It is observed that in the given situation both the TE- and TM–mode reflection coefficients are fairly frequency independent for permittivity values in the second medium that lie between 8 and 16 for frequencies above 200 MHz. Generally speaking, the TE-mode reflection strength is one order of magnitude smaller than the TM-mode reflection strength. The reflection strength is primarily determined by the contrast in permittivity leading to large reflection amplitudes (low attenuation) with increasing permittivity. The results in Figure 5b and 5d show the attenuation due to TE and TM reflection amplitudes for the same electric parameters for layer 1 and for a fixed electric permittivity in layer 2 of $\varepsilon_{r;1}$=20 and for conductivity values that range from σ=0.001 S/m (fresh water) up to σ=1 S/m (sea water) plotted on a logarithmic scale. It is observed that the reflection strength is only dominated by conductivity for conductivity values in the second medium that are above 0.3 S/m (values of 0.5 on the logarithmic scale). In those situations, the reflection strength is large because the reflector acts almost as a perfect reflector. For all conductivity values considered, both reflection coefficients are frequency dependent, which frequency dependence reduce drastically for much higher frequencies we would normally consider in asphalt pavement applications. From a certain frequency onwards the attenuation becomes frequency independent and

The signal return from flat interfaces that separate two homogeneous layers is well-described by these formulas and hence the figures are a realistic representation of what can be expected in terms of recorded amplitude. Of course, real dam and road asphalt structures are not homogeneous layers and also the boundary separating two layers is not flat. The words "homogeneous" and "flat" have a meaning only in direct relation with the scale of the waves that are used to probe the layers. In case the wavelength is large compared to the heterogeneities, the medium can be regarding as an effective homogeneous layer. This implies that a constant velocity can be used but that an extra attenuation factor is introduced due to scattering loss. Scattering loss is a term related to the omni-directional reflection of wave energy by obstacles. Scattering loss is directly related to incoherent arrivals at the receiving antenna and it obscures the coherent reflections off target objects. So there is an additional loss term in the effective medium parameter and the scattered energy (clutter) overlaps coherent arrivals. The asphalt

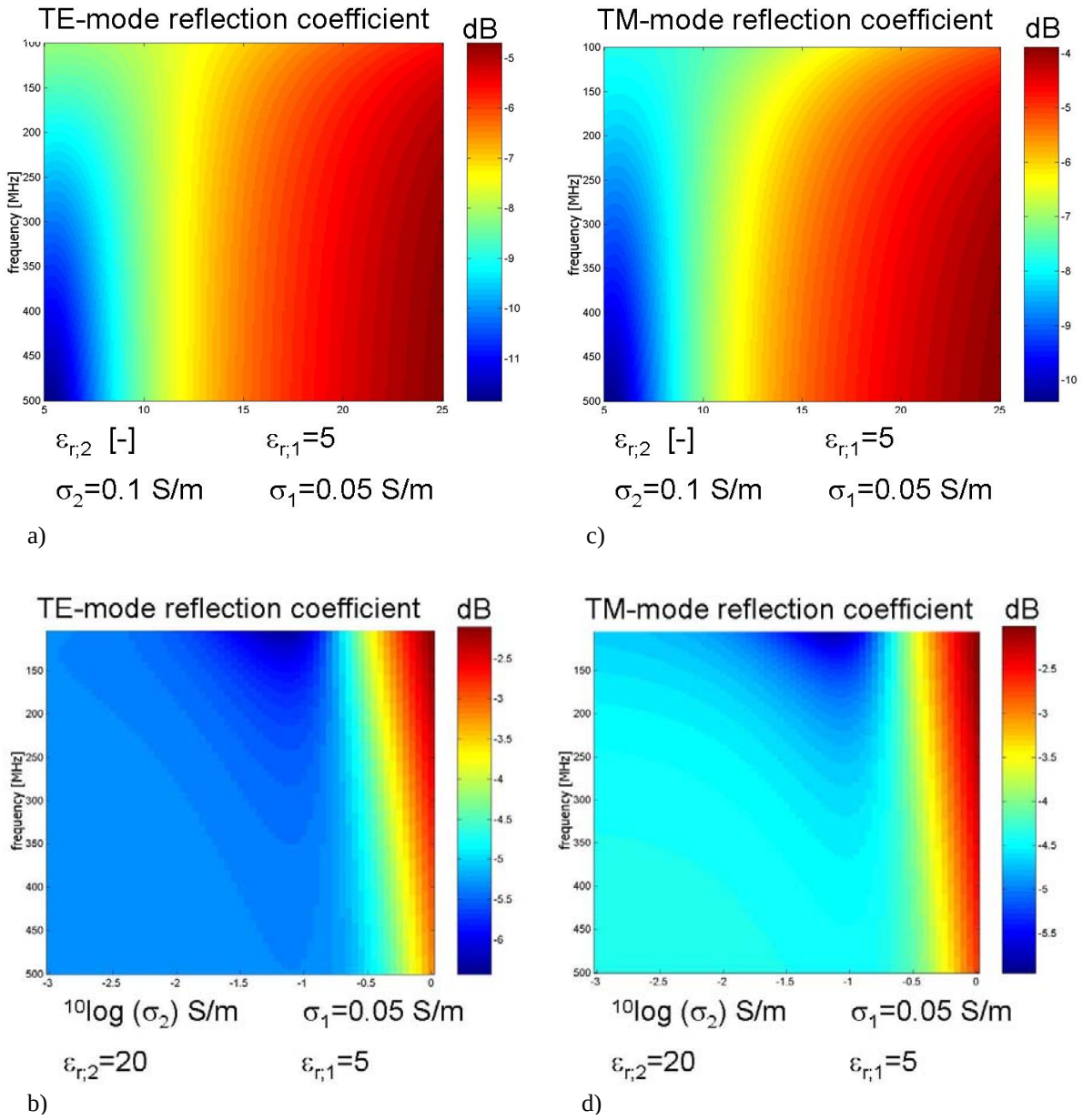

Figure 5: TE- and TM- mode attenuation as a function of frequency and relative electric permittivity in the second medium (a and c) and on a logarithmic scale as a function of electric conductivity in the second medium (b and d).

constructions under consideration are large collections of obstacles that are bound together by bitumen. Collections of obstacles introduce large amounts of scattering because these obstacles start to interact with each other. This makes it hard to interpret GPR reflection data in these environments. The clutter level is increased by increasing the frequency of operation, for which reason the penetration depth decreases with increasing frequency. When an obstacle is disturbed by a wave it becomes a secondary source and starts to radiate electromagnetic waves. When the obstacle is small compared to the wavelength of the impinging wave it can be regarded as a point source, which is omni-directional. When the size of the obstacle is in the order of the wavelength then it has a cross-scattering ratio value that is less than 1, and still scattering loss occurs because not all energy is reflected and some energy is scattered. When the lateral size is of the order of the first Fresnel zone it behaves as a reflector without introducing scattering loss. Now for interfaces we must look at the surface irregularities. Here we use Rayleigh's scattering criterion, which states that when surface irregularities are smaller than the wavelength divided by eight ($\lambda/8$), the surface can be regarded as flat. When the irregularities are larger, one can no longer speak of an interface and scattering loss has to be introduced when still the reflector description is used. Hence the occurrence of irregularities in a surface or interface reduces the penetration depth further and the effect increases

with increasing frequency. On the other hand, a certain change in the clutter level in GPR data is a direct indication that something has changed in the structure of the layer and may lead to the detection of layer integrity loss.

2.3 Acquisition and processing

Now that we have information on the frequency band, the associated wavelengths and expected attenuation and dispersion along the travel paths, and the effects of reflection and transmission, we define general rules for minimum requirements for the acquisition parameters that will allow data processing procedures for optimizing the information return from the measured data. First we give here the radar range equation

$$P_R = \frac{P_T \sigma \left(\lambda/\varepsilon_r\right)^2}{\left(4\pi\right)^3 R^4 L_p}$$

which is a frequency domain expression and where P_R = received power, P_T = transmitted power, σ = radar cross section of the target (reflection coefficient times distance squared for a plane interface), λ = wavelength, ε_r = dielectric constant, and R = distance to target. The maximum range is considerably influenced by the path loss Lp(λ) and P_R must be above the minimum detectable signal level of the system. In the previous sections all these parameters have been defined and explored for the typical variety of asphalt constructions.

Granular materials, like bituminous asphalt concrete, are complex electromagnetic media, because the gravels or road material in general with which the main layer is constructed is a porous medium that must be probed with waves whose length is at least an order of magnitude larger than the size of the stones. If shorter wavelengths are used, scattering from every single piece of stone will result in a blurred dataset. There is a large amount of information in such data, but present day technology has no means to extract the information and we regard it as noise or clutter. This limits the upper frequency that can be used. If much higher frequencies are used, the method will be similar to photography and clear images can be made of single particles or cluster of particles below the surface, depending on the wavelength.

We assume a relative permittivity varying from 2 to 25 for asphalt concrete where the porosity can change from 5% to 50% (dense to porous) and pore fluid can vary from air to water, with some mixtures of sand, water and debris in between these extremes, see Figure 6. The most reliable mixture rule for air or water filled porous media is the so-called complex refractive index model (CRIM), given by

$$\sqrt{\varepsilon_{r,\text{eff}}} = \sqrt{f_{\text{solid}}\varepsilon_{r,\text{solid}} + f_{\text{bitum}}\varepsilon_{r,\text{bitum}} + f_{\text{water}}\varepsilon_{r,\text{water}} + f_{\text{air}}\varepsilon_{r,\text{air}}}\,, \tag{8}$$

Where f_{solid} is the volume fraction occupied by the solid granular material in the asphalt, etc., and hence the total sum of all volume fractions equals unity. For propagating waves with a wavelength larger than the grain sizes this is an accurate formula. We use a fixed ratio of grains and bitumen of f_{solid} / f_{bitum} =88/12 occupying the non-porous space and the pore volume given here is the effective pore volume after the pavement has been laid down. If porosity is denoted by φ then we have f_{solid} + f_{bitum} =1-φ, while f_{water}+ f_{air} =φ. Water saturation is then defined as Sw= $f_{\text{water}}\varphi$. We have used relative permittivity values of 1, 2, 5 and 80 for air, bitumen, grain and water. Using other numbers will change the result. For air the value is fixed and for water at 20 ^{o}C the value of 80 is accurate. The other two numbers depend on the material used but will not differ very much from the values used here.

In Figure 6 we show the square root of the relative electric permittivity, because this is the number with which the free space wavelength has to be divided by to find the wavelength inside the pavement, which determines the amount of scattering and range resolution. Given a frequency range from 500 MHz to 3 GHz, the wavelength at the smallest value of the relative permittivity ranges from just below 43 cm at low frequencies to just over 7 cm at high frequencies. At the highest value of the electric permittivity at ranges from 12 cm down to 2 cm. If the whole bandwidth of 2.5 GHz is available, the resolution ranges from 6 cm at the lowest permittivity value to 1.7 cm at the high permittivity value, which in both cases corresponds almost to the smallest wavelengths at the given permittivity values. For pulsed systems the amplitude spectrum over the available frequency band is not flat, implying that for pulsed systems the resolutions is less. For time domain wide band systems usually the dominant frequency is used as a measure for the resolution. At a 2 GHz dominant frequency time domain system the resolution would be the same as for a frequency domain system with a flat amplitude spectrum. At lower dominant frequencies.

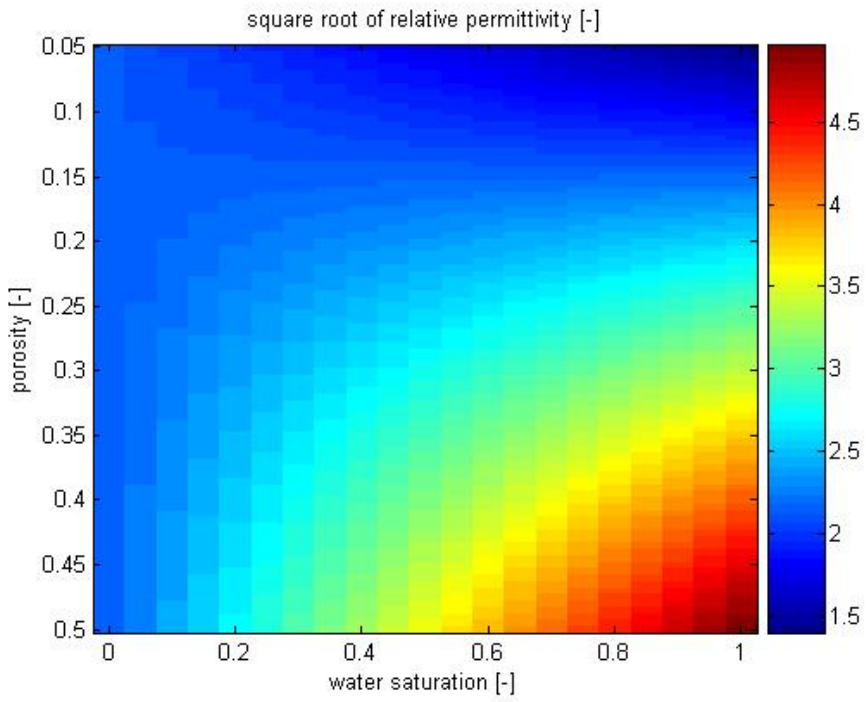

Figure 6: The square root of the effective relative electric permittivity is shown as a function of water saturation and porosity.

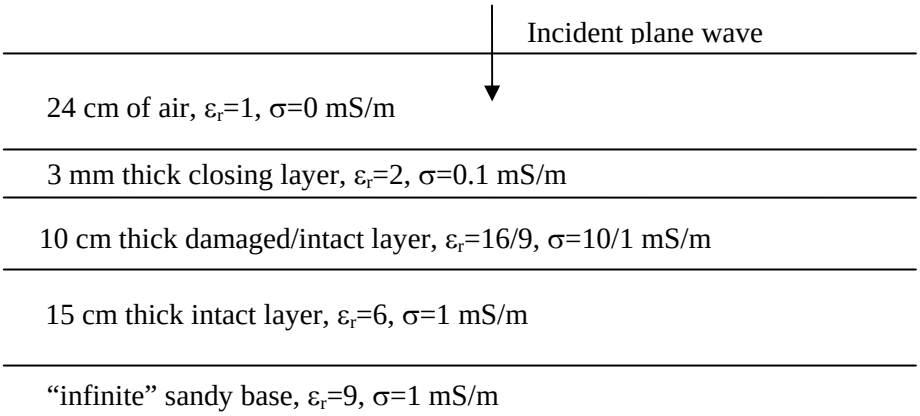

Figure 7. Example configuration showing expected measured responses when a normal incident plane wave is used as excitation on a model layered system including a thin closing layer of bitumen followed by a damaged layer below which an intact layer is present over a homogeneous half space of sand. The damaged layer is also modeled as an intact layer, in which case it has the same properties as the layer below it.

As an example a simple four layered earth is used as a model for a pavement layer on a sandy base as indicated in Figure 7. The excitation mechanism for the model is a normal incident plane wave at different frequency values such that both a frequency domain system and several time domain systems can be modelled to show the effects of the different systems and the effective frequency bandwidths they use. The layer below the first thin layer is a damaged layer that is also used as an intact layer to compare the differences in the reflection response. The third layer is an intact asphalt layer and is followed by a homogeneous half space sand.

In Figure 8 the time and frequency domain signatures are shown of an example source wavelet, which is indicative for the wavelets emitted by the antennas from GSSI. As indicated in Figure 8, a bandwidth of 2.5 GHz the center or dominant frequency of 2 GHz is just feasible, while the bandwidths at lower center frequencies is smaller.

Figure 9 shows the amplitude and phase spectra of from 4 MHz to 5 GHz of the layered model given in Figure 7 of a damaged asphalt concrete layer on the left and the fully intact layer on the right, including the thin top bituminous layer of 3 mm. The phase spectra show abrupt changes that are caused by the definition of phase by its principal value being in between $-\pi$ and $+\pi$, the overall behaviour is linear, indicating a single half space. In the oscillations of the left amplitude plot compared to the right plot, it is directly visible that more layers are present in the left plot than in the right plot. In the left plot the main oscillation has a repetition of about 375 MHz and it is superposed on an oscillation with a lower frequency and one with a higher frequency. In the left plot the dominant oscillation occurs at 170 MHz. The interesting feature of the phase spectra is that they are quite similar and only differ in the subtle changes relative to the overall linear behaviour. These deviations from linear behaviour indicate that there are changes in the medium, because the phase spectrum would be exactly linear for a homogeneous half space below the surface. It can be concluded that both the amplitude and phase spectra contain important information about the layered system. It is noted that the spectra shown here are not weighted by the amplitude spectra of the source signature used. In that sense these spectra correspond to the measured spectra for a frequency domain system. For a pulsed system, only the pulse shape with a center frequency of 2 GHz would show this information clearly.

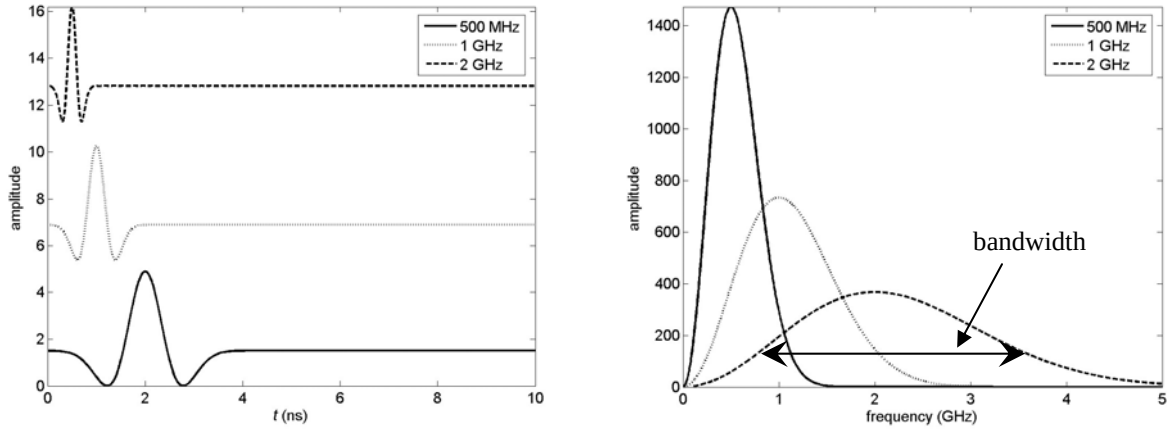

Figure 8. In the left plot the three time signatures of the source wavelets are presented and their corresponding frequency domain amplitude spectra are shown in the right plot.

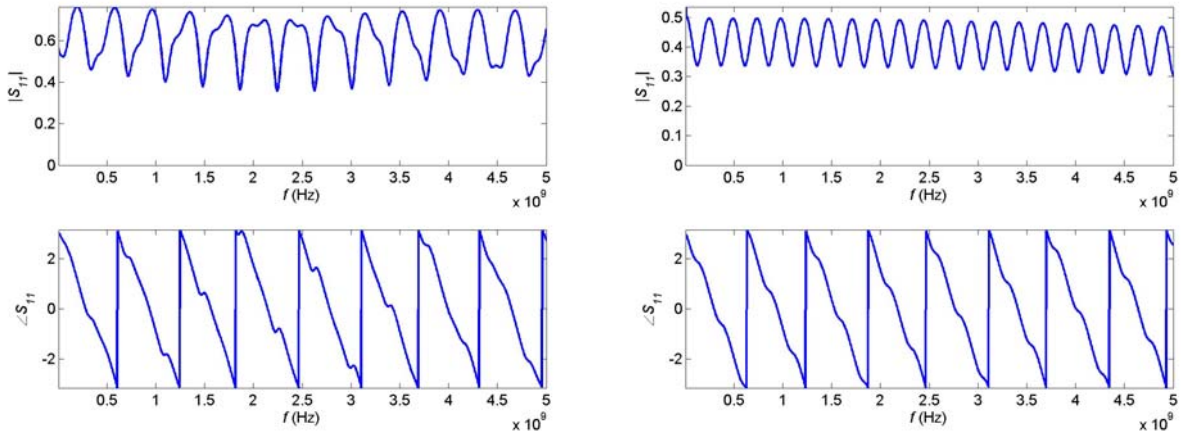

Figure 9. Amplitude (top) and phase (bottom) spectra from virtually zero frequency to 5 GHz of the model with damaged layer (left) and completely intact layer (right).

Figure 9 shows the time domain reflection responses of the weighted spectra using the three different source time signatures as given in Figure 8. These then represent actual time domain results of pulse systems that would operate in the bandwidths used here. The model with the damaged layer is shown in the left column and the intact model response is presented in the right column for wavelets with dominant frequencies of 500 MHz, 1 GHz and 2 GHz from top to bottom, respectively. There are several important observations to be made. First we have

assumed that the source generating the incident wave is located 24 cm above the surface and the first reflection event, with the largest amplitude is the combined reflection from the surface and the bottom of the bituminous layer of 3 mm. Since the contrast between air and the thin top layer is very small, its presence is hardly visible. A strong contrasting thin layer would lead to a large number of multiple reflections within the thin layer that all arrive well before the first reflected wave has completely returned to the receiver and which leads to a dispersed signal. The clean signal shows there is no thin high contrasting layer. Then it can be observed that with a center frequency of 500 MHz it is not directly clear from the data that there is a separate layer, although it is just barely visible. Yet all the information is there and can be retrieved using mathematical models. At higher center frequencies one has no difficulties identifying the separate layers. This does not lead to the conclusion that there is a damaged layer. The change in polarity of the reflected signals does indicate that there is first an increase in permittivity followed by a decrease, indicating a damaged layer in case it is partially water filled. The fact that the third reflection response is the first event whose pulse shape is not symmetric indicates that the second layer has a relatively high conductivity, indicating water with some dissolved solid particles, which usually occurs with partially or fully water saturated porous granular material. When the antennas used are well calibrated, it is possible to perform numerical inverse analysis, retrieving the complex electric permittivity as a function of depth, on a single data record (called trace) and subsequent analysis of several traces can lead to sound interpretations.

When the antennas cannot be properly calibrated no true quantitative information is known and one has to go to other methods of data processing and interpretation. This usually occurs with ground coupled antennas, where the antenna performance is primarily determined by the impedance (mis)match to the ground surface. Then quantitative analysis can be performed by performing multi-offset measurements and perform a velocity analysis. If this is not possible or desired, one can always try statistical methods and qualitative interpretation by looking for changes in the reflection responses and checking them with the ground truth. The experience built in this way can also be used successfully.

The ability of information retrieval from acquired data is mostly determined by correct acquisition and knowledge of the crucial parameters. The important parameters are position of the antennas at each measurement location, orientation and polarization of the antennas. The location can be controlled by using a odometer and the assumption that the recordings are made along a straight line. This assumption can be dropped when the line along which the recording is made is measured or forced through an independent measurement. An example of this is given in Lualdi *et al.* (2006). The full position and orientation information can be retrieved by measuring the position of the antenna in three-dimensions at small time intervals. By following a track of the antennas one can compute the position, inclination and azimuth of the antennas at each measurement location. An example is given in Lehmann and Green (1999), although the authors use their information only to know the antenna position. The importance of accurate position and orientation information is underpinned in Slob *et al.* (2003), who show that a lot of so-called clutter is the remaining energy due to imprecise focusing because of incorrect position information used in the imaging procedure. Knowledge of the propagation velocity and its distribution in the subsurface is necessary to translate recording time to physical depth.

The most reliable way of estimating subsurface velocities is by recording several traces with a fixed mid point and increasing symmetric distance between the transmitter and receiver antennas, see Figure 11. Since many traces are recorded at known horizontal distances, the unknowns are velocity distribution in the ground and the depth to a reflector. If the reflector is dipping, the dip of the reflector can also be inverted for. If only data with a fixed distance (common-offset mode) between the transmitter and receiver is recorded no direct way of determining subsurface velocity is available. In the fortunate situation that a clear reflection occurs in the data that comes from a small object, where is small is relative to the wavelength in the ground, then a velocity estimate can be obtained, see Figure 12, on the condition that the visible reflection hyperbola is well-sampled, which term is explained at the end of this section. When off-ground antennas are used the reflection coefficient of the surface can be used to estimate the permittivity changes as a function of depth when the recording is normalized by a recording over a metallic plate, which is modelled as a perfect conductor. Then it is important to keep the height of the antenna fixed for all measurements and equal to the measurement over the metal plate. This way of recording and processing will produce an estimate of permittivity as a function of depth, which produces then also a layer thickness estimate. The advantage of this method is that the changes in electric parameters is also an indication for layer quality in some sense, primarily determined by the amount of water present in the layer, which can be an important quality parameter. The disadvantage of this method is that the accuracy of the result is quite sensitive to height differences in the measurement relative to the measurement over the metal plate, Lambot *et al.* (2006). This problem is circumvented when the more elaborate antenna calibration procedure is carried out as described in Lambot *et al.* (2004). The height of the antenna is an unknown parameter that is also inverted for. This increases

the accuracy of the model to the processed data of each measurement to the degree that also an estimate of electric conductivity is possible with an accuracy better than an order of magnitude.

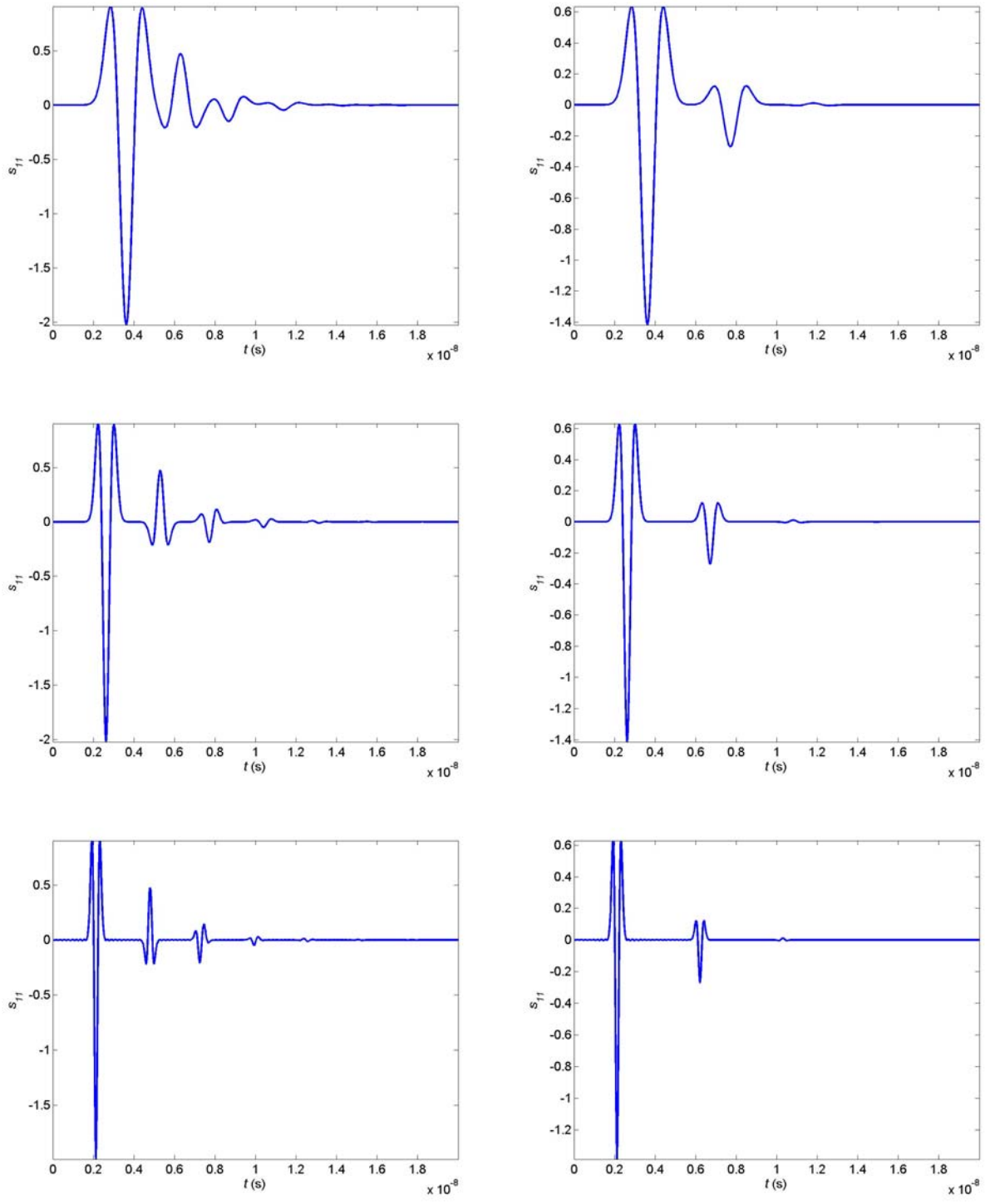

Figure 10. The time domain reflection responses of the model of Figure 6, using the source time signatures of Figure 7 with center frequencies of 500 MHz (top), 1 GHz (middle) and 2 GHz (bottom) for the model containing a damaged second layer (left) and a full intact layer (right).

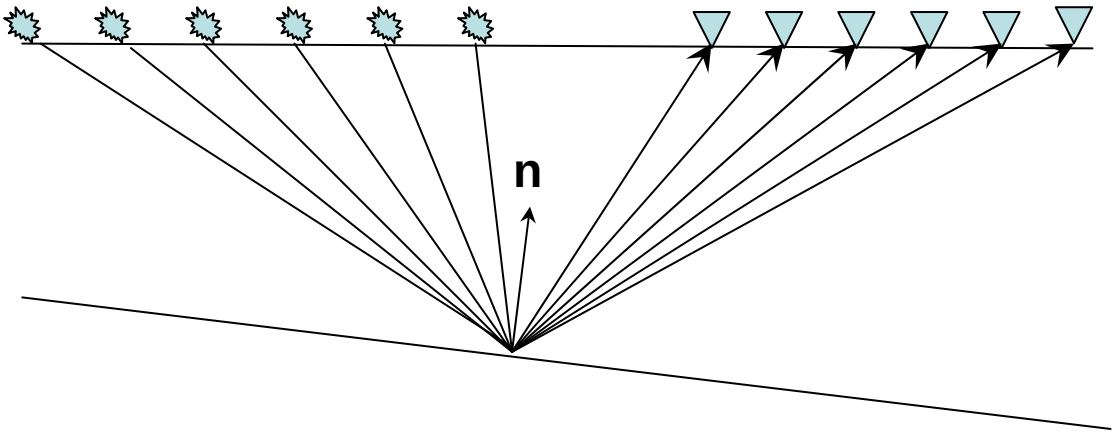

Figure 11. Schematic drawing of a CMP measurement configuration for a dipping reflector from which data accurate estimates can be obtained about the direction of the normal vector **n**, the velocity of the propagating waves in the layer between the surface and the dipping interface and depth to CMP point.

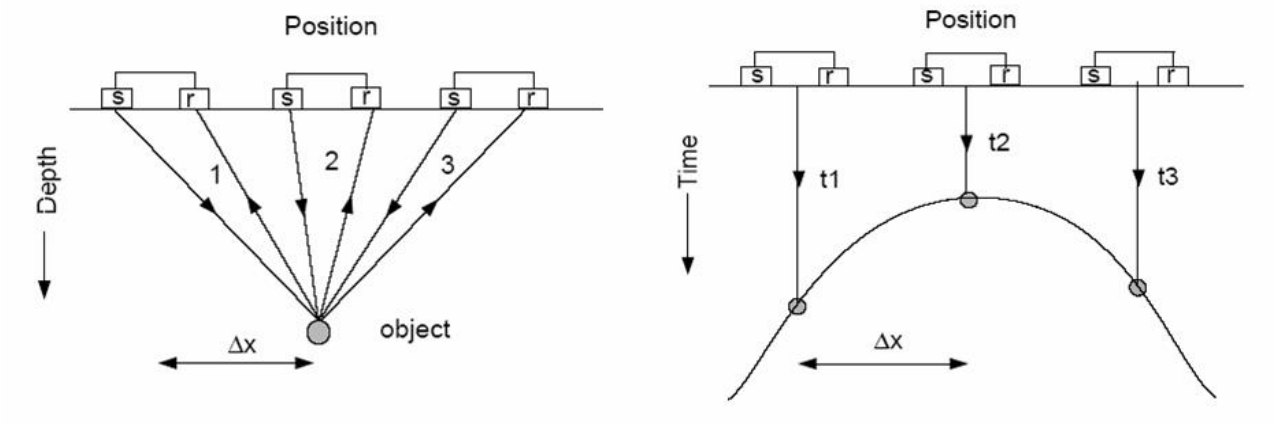

Figure 12. Hyperbolic type reflections from an object in common-offset mode.

This brings us to the question: What do we mean with "well-sampled"? From signal analysis it is known that a wave of which at least at two locations within a single wave length a sample is taken, can by completely and exactly reconstructed, which is known as Nyquist's criterion. For waves propagating under an angle relative to the locations of the receivers, the apparent wavelength should be used as a measure for determining the maximum distance between two receiver locations on the surface, see Figure 13. For horizontally travelling waves, the criterion is the strictest. When the depth of investigation is small this is the best way to determine maximum spatial sampling distance. For a given frequency the smallest wavelength corresponds to the lowest propagation velocity and for a given velocity the smallest wavelength corresponds to the highest frequency. To ensure unaliased data recording in space the highest frequency of operation should be taken with the expected lowest velocity. In the example given in Figure 10, where the smallest velocity is 7.5 cm/ns and the highest frequency is 5 GHz, the distance between two adjacent measurements on the surface should be less than 7.5/10=7.5 mm. If we reduce the maximum frequency to 3 GHz, the maximum distance between two receiver locations is 1.25 cm. If larger distances are taken, the scattered events coming from depths within the first wavelength may not show up as coherent events and may not be recognized as reflections from an object or irregularity in the shallow part of the subsurface but could be regarded as clutter, or incoherent scattering. This will greatly complicate the interpretation of recorded data over asphalt layers where the damaged zones are within the first 5 to 10 cm below surface.

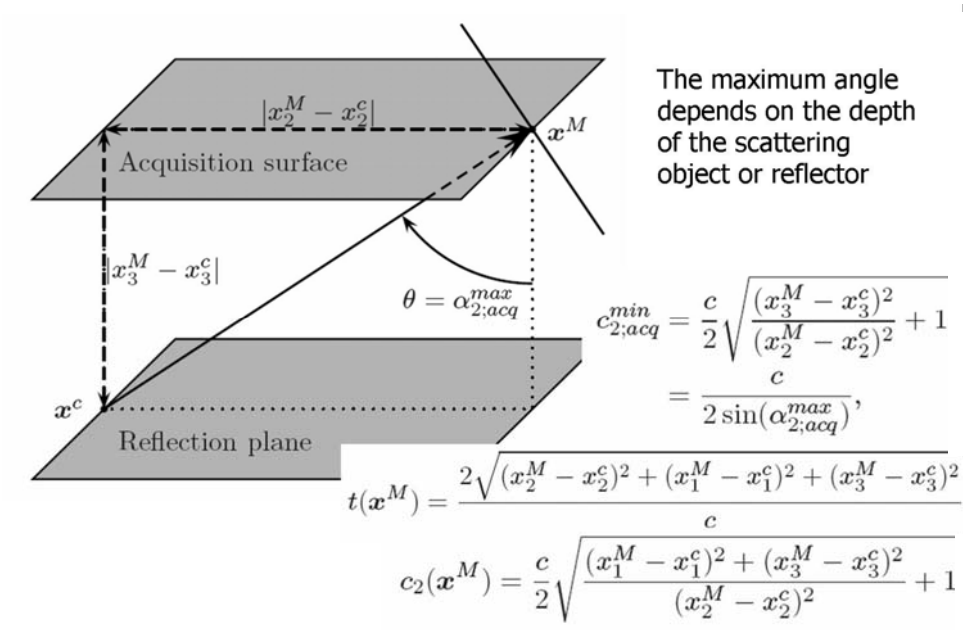

Figure 13. Some criteria for acquisition geometry design. The apparent velocity $c_{2;\mathrm{acq}}^{\min}$ should be used with frequency to determine the wavelength seen be the receivers, x^M is the midpoint coordinate between the antennas and x^c is the point at the target furthest away from the antenna.

3 Case histories and test results

One of the world largest outdoor pavement laboratories is the Minnesota Road Research Project. It has a vast electronic sensor network (over 4500 sensors) embedded in six miles of test pavements and is located 60 km north of Minneapolis/St. Paul. The sensor network and data collection system provides ample opportunities for studying the effect of heavy traffic, heavy rainfall and annual freeze thaw cycles on the pavement materials and designs. In the late 1990's several tests have been run with air-launched and ground-coupled antennas. It was concluded that air-launched horn antennas are very suitable to determine a vertical profile estimate of electric permittivity. This profile was successfully used to determine layer thicknesses on different kinds of road structures and layer quality related to uptake of water and salinity. Stripping, voids and moisture anomalies were also successfully detected. In Minnesota the excess of moisture in the unbound base layer that was detected by GPR, proved to be the major contributor to pavement failure. For stripping GPR data results were compared to the falling weight deflectometer (FWD) deflection bowl data and from the combined analysis of a few drilled cores, the deflection bowl data and GPR data it was possible to make a reliable division into four classes of stripping, from no stripping, light/early phase, medium to severe stripping. The company Roadscanners has performed these tests and they have developed a software package called Road Doctor ©. Independent work from the Texas transportation institute together with the Florida department of transportation has lead to a similar computer program called TERRA.

Since the mid-1990's Hugenschmidt has done a lot of work in Switzerland on motorway pavements. He came to the main conclusion that GPR proved a valuable tool to complement existing monitoring methods of pavement distress and planning of repair work. Previously unknown damaged zones were detected and the horizontal extent of known zones were accurately determined as well as the varying depths of the problem zones in the pavement layers were resolved. He found it was essential that the GPR interpreter and a pavement engineer, performing visual inspection, worked together. The GPR was found to be a suitable tool for quality control by using the GPR before and after rehabilitation work.

Similar to the work in Minnesota, there is a central laboratory of bridges and roads (LCPC) in Cedex, France, which is a state research organization working for the state and local authorities. They have large test facilities, one of which is a circular pavement fatigue test track, which is ideally suited for GPR work. They have done several GPR

test evaluations in the late 1990's and found that the CMP method is the most accurate method for layer thickness determination, without having the need for calibrating their results with a drilled core. They have developed a numerical inversion code for multi-offset air coupled antennas.

The universities of Rome, Italy, and Liverpool, England, develop methods relying on stochastic models and neural networks for moisture prediction in road pavements.

During the last decade the Geotechnical Research Group (HTTI, Korea Highway Corporation) in Korea has done a lot of work on testing GPR on road settlements on soft grounds. They use air-coupled antennas and calibrate with recording the reflection from a metal plate and obtain reliable results in layer thickness determination and can easily find the locations where the pavement has excessive thickness due to uneven settlements and can relate this to the thickness of the soft ground and the period since it has been open to traffic.

In 2005 a large study was published by several people from different institutes in the USA (Grote et al. 2005), who concluded that an estimate of moisture content, with an absolute accuracy of 0.02 m3/m3 in sub-asphalt aggregate layers, can be obtained with GPR data and that GPR can be used for assessing pavement drainage layer efficacy. All pavements they tested on were laid according to the California department of transportation specifications and consisted of drained and undrained pavements. They used 900 MHZ and 1200 MHz ground coupled antennas and used 2 cm spacing between measurements controlled by an odometer wheel. The 900 MHz antennas were in multi-offset mode from which analysis velocities were determined. The test results come from controlled infiltration experiments and both types of asphalt layers.

The group of researchers in the Third University of Rome, Italy have used road degradation classification catalogues from Hong Kong, France, US and Switzerland that include specific damages that are distinguishable electrically. These are point defects (e.g. voids, small water inclusions, longitudinal and branched cracks), along road long wavelength defects between different layers (e.g. depressions, or stresses due to differential settlement) and along road short wavelength defects between two layers (e.g. pumping of subsurface water into the layer, localized subsidence). There are internal (due to faults in the construction) and external (due to ground properties and changed conditions) causes of these damages. This group employs a simplified model of the expected recordings and uses different numerical algorithms to detect and characterize pavement damages. The algorithms are applied to GPR data from 600 MHz and 1.6 GHz center frequency ground coupled bow-tie antennas. The algorithms allow for computing confidence bounds and they conclude that horizontal spatial correlation properties can be used as a measure for the pavement damage problem.

A Summary of the results from the above work for thickness evaluation is given in Table 1. For integrity evaluation no such table can be made with a clear and justifiable average or overall conclusion on accuracy.

Table 1. Summary of tests published in the literature of GPR performance in road pavement thickness evaluation.

antenna	Calibration	description	advantages	disadvantages	accuracy
Air-launched	Drilled cores	Freq. domain, Tracks lateral continuation	no special knowledge required, UWB	Slow, uncertain results	qualitative, depends on amount of change
Air-launched	Base plate	Freq. domain, Num. inversion each trace	Fast, UWB	Slow, calibration height of antenna should be maintained, special knowledge required for numerical inversion	Variable, depends on stability of antenna height
Air-launched	Full system	Freq. domain, Num. inversion each trace	reliable, UWB	Slow, special knowledge required for numerical inversion	~5% error
Air-launched	none	Pulsed system	Fast, no special knowledge required	limited bandwidth, calibration height of antenna should be maintained, special knowledge required for numerical inversion	qualitative
Air-launched	Base plate	Pulsed system	Fast	limited bandwidth	Variable, depends on stability of antenna height and on presence of thin near surface layers
Air-launched	Full system	Pulsed system	Fast, reliable	limited bandwidth	~10%, depends on presence of thin near surface layers
Ground-coupled	Core drillings	Single channel Freq. domain	UWB	Slow, in case CMP data is collected: very slow	qualitative
Ground-coupled	None	Multi-channel Freq. domain	UWB, layer thickness from velocity analysis	Slow, or expensive	~10%, depending on layer homogeneity, thickness and resolution
Ground-coupled	Core drillings	Single channel pulsed system	fast	limited bandwidth	qualitative
Ground-coupled	None	Multi-channel Pulsed system	fast, layer thickness from velocity analysis	limited bandwidth	~10%, depending on layer homogeneity, thickness and resolution

4 Acoustic and seismic methods

The table below comes from evaluations of the Innovative Pavement Research Foundation, which issued the report in May 2006 (Report IPRF-01-G-002-02-2). The report describes acceptance criteria for airfield concrete using seismic and maturity concepts. Ultrasonic impact-echo techniques are used and seismic surface waves are used, both with a given error bound of 5%.

The American 'Committee on Strength and Deformation Characteristics of Pavement Sections' has written a communication in the late 1990's, which states: "As we move into the next millennium two prime issues face researchers. The first is related to building an implementation framework. The challenge is how to take complex and sophisticated laboratory testing, and performance prediction models, and implement them as routine

procedures within the pavement design community. The first step toward implementation involves clearly demonstrating the benefits of the proposed improvements over existing methods for the variety of materials and pavement types designed. The second challenge is ensuring that the procedures are practical and can fit within the organizational and time constraints under which pavement designers' work. The second challenge involves integrating the laboratory and NDT equipment so that the same set of pavement properties is used in all phases of pavement design, quality control monitoring, and performance evaluation."

Table A.2 - Summary of Tests Used to Determine Concrete Strength

Test Method	Description	Advantages	Disadvantages	Accuracy
Compressive Strength (ASTM C39)	Cylindrical concrete specimen is subjected to axial compressive forces and loaded to failure.	• Standard test method with long history of use in acceptance testing. • Relatively easy test to conduct.	• Test is not representative of the typical stress conditions which cause PCC pavements to deteriorate. • Some effort is required to prepare specimens in the field and transport them to the lab for testing. • Differences between lab and field curing conditions.	--
Flexural Strength (ASTM C78)	Rectangular beam subjected to bending under third-point loading until failure.	• Standard test method with long history of use in PCC pavement design and evaluation. • Test is representative of the typical stress conditions which cause PCC pavements to deteriorate.	• Beam specimens are relatively heavy and bulky. • Significant effort is required to prepare specimens in the field and transport them to the lab for testing. • Differences between lab and field curing conditions.	--
Maturity Method (ASTM C1074)	Accounts for the combined effects of time and temperature on strength gain. Method involves pre-construction testing of the concrete to establish the maturity relationship.	• Fast and simple nondestructive test method. • Accounts for in situ curing conditions.	• Determination of maturity relationship requires significant up-front effort. • Strength-maturity relationship is mix specific.	As yet to be established.
Ultrasonic Pulse Velocity Method (ASTM C597)	A nondestructive, sonic-based approach used to measure and analyze the speed of ultrasonic waves generated in concrete, which can be used to estimate the dynamic modulus of elasticity and strength.	• Fast and simple nondestructive test method. • Accounts for in situ curing conditions.	• Many variables can affect velocity measurements (moisture, steel, aggregate type/size, non-homogeneity of concrete). • Strength-pulse velocity relationship is mix specific. • Appropriate sensor configurations required (direct and semi-direct preferred). • Sensors must have good acoustical contact.	~5%
Seismic Method	Utilizes seismic surface wave velocity to estimate dynamic modulus of elasticity (which can be related to strength).	• Fast and simple nondestructive test method. • Accounts for in situ curing conditions.	• Strength-pulse velocity relationship is mix specific. • Sensors must have good acoustical contact.	~5%
Integrated Seismic-Maturity Method	Incorporates both the concrete maturity and seismic analysis technologies to accurately determine concrete strength and pavement thickness.	• Fast and simple nondestructive test method. • Accounts for in situ curing conditions.	• Strength-pulse velocity relationship is mix specific. • Sensors must have good acoustical contact.	--

From this we conclude that there is no routine procedure for road pavement analysis using seismic/ultrasonic methods. The seismic surface weave method is still in a research state and other more sophisticated techniques have been developed for other problems, some of which could be used for pavement evaluation. Another reason is that these methods are in a research state.

The falling deflection method can be understood as a seismic method where the falling weight is the source of seismic energy and the recorders are geophones that measure the vertical particle velocity component.

Because pavement integrity is a mechanic property, changes in this property to the extent that a layer is considered as being of bad quality is a mechanical property that should in principle be detectable by mechanical methods, like the seismic method. Delft University of Technology is interested in investigating two main targets for application of modern seismic technology: 1) thickness of the top protective layer 2) spatial variation in the consistency/tightness of the bulk material constituting the top protective layer.

The seismic investigation will then start with the performance of a walkaway noise test. The objective of this test is to determine the correct aperture and the samplings in time and space for the seismic acquisition. The desirable seismic reflection events, alignment and velocity of surface wave trains, indication of any lateral change in seismic velocity, will be looked into using one or two shot gathers containing many receivers. Both P and S wave sources and horizontal and vertical receivers will be deployed. This procedure defines the seismic acquisition parameters that will be then be used to conduct the seismic profiling. Next, a seismic reflection shooting over a characteristic length (e.g. about 50 m) must be performed, so that the final processed profile length (with sufficient CMP fold) is of the same size as the characteristic length. A test measurement will be carried out in September 2006 in Zeeland to assess the success of this method in achieving the above two goals.

Other interesting seismic techniques exploit the scattering from near surface heterogeneities that require three-dimensional acquisition and will therefore only be efficient when seismic landstreamers can be used. (Riyanti et al., 2005, Campman, *et al.*, 2006). The described techniques are very suited for finding mechanically degraded zones.

5 Discussion and Conclusions

In this report a literature study is described of the modern approaches with regard to asphalt pavement applications ranging from layer thickness determination to the detection of degraded zones. In the public domain, all publications in this context use GPR equipment and no account was found where modern streamer seismic receivers were used together with seismic sources dedicated to shallow investigations. Nevertheless interesting techniques exist that could be used efficiently when land streamer would be used and which are very suited for finding mechanically degraded zones.

Seven GPR equipment manufacturing companies are listed (Refs. 40 -49), most of which sell special GPR units dedicated for use in asphalt pavement investigations. These are commercially available products. Three service companies are listed. Allied-Associates (Ref. 40) is an English based company with branches in Germany and Belgium and operates equipment from GSSI (an OYO corporation company). Aperio (Ref. 41) is an English based company and work with GSSI equipment, while T&A Survey (Ref. 42) is a Dutch based company and works with Sensors and Software equipment. All three use ground-coupled antennas, but Refs. 40 & 41 also use air-launched antennas for network pavement applications. There are undoubtedly many more companies offering similar works for pavement applications and my search has certainly not been exhaustive.

From the public domain publications, it can be concluded that from theoretical considerations and in all reported studies, GPR can be used successfully to determine asphalt layer thicknesses and zones of degradation can be detected when water has infiltrated the asphalt layer pore space. Layer thickness determination has always proven possible and accurate when the GPR system was properly calibrated. Calibration is preferably done by calibrating the antennas and system, followed by parameter inversion to determine layer property and thickness, but can be done using drilled cores. The location of these cores should then be made based upon assessment of the GPR data. The simplest configurations use air-launched antennas, but ground-coupled antennas can be used as well. Multi-offset antennas used in multi-channel systems provide additional information, which can be used to compute and improve confidence intervals on the obtained results. Probably the most experience in this respect lies with the company selling such a system (Ref. 46).

A small theoretical investigation presented here to put a lower bound on usable frequencies shows that from 500 MHz upward GPR should provide excellent data for several applications in asphalt concrete road decks and other types of pavement, even in the extreme environment of sea dykes. The highest frequency from which coherent reflections can be expected depends very much on the size of the grains that are used in building the asphalt layer; the wavelengths used must be larger than the size of the grains. On the other hand, lateral changes in the clutter profile are a direct indication of changes in the pore space. These can be geometrical or because of changes in the pore content, or both.

There is one paper on the use of multi-offset data, but no account was found on using multi-offset multi-channel GPR systems for pavement evaluation. A technique that has not been used, but could be investigated uses dispersion curves that are used in waveguide investigations. These allow accurate estimation of a very thin top layer, where thin is meant relative to the used wavelengths and this method is sensitive to lateral variations inside the thin layer, which analysis has been described for geophysical radar application by Kruk *et al.* (2006). If a degraded layer would be overlying an intact layer a waveguide is present and can be evaluated with the above described technique.

Since I have searched the public domain literature no commercial procedure can be reported on. The reason is that private domain knowledge is not free and there has been no budget to purchase private knowledge. There is no way of knowing what the state of the art is. If companies cannot be open, for whatever reason, about their procedures, it is impossible to know or even guess what they do. For the author this leads to unacceptable uncertainties. It should be no problem for a company that wants to sell its business to refer to published works as an indication of their capability. All methods described above are at some level of research. This implies that methods and techniques that have been found successful in layer thickness determination and layer damages on a wide variety of pavement structures, require careful planning and execution of the acquisition and a lot of work after the data has been collected to arrive at good results. This makes the techniques rather expensive at the present level of development. Once these methods have been further developed to a higher degree of automation, the cost can be made substantially lower. This requires more work and is open for the future. It is certainly clear

from the all studies mentioned that simply interpreting collected GPR data in fixed-offset mode only is not sufficient to arrive at acceptable results.

To make a cost estimate now, I would say that the price of a commercially available GPR system would be around 50 k€. This is virtually independent of system and antenna configurations. It is possible to build a custom GPR , for around 10 k€, but that would at this moment be slow compared to the commercially available GPR systems and hence not cost effective. To collect data can vary from several km's per day to just 1 km depending on the equipment and the goal of the survey. For some problems it is better to collect data in a number of parallel lines for three-dimensional processing and inverse modelling or to make plan views of the processed data. Depending on the type of system one or two persons are required to collect the data. The processing, inverse modelling and interpretation of the results can vary a lot depending on the survey size and goals, from one day (for manual processing and interpretation of a small survey to automated processing and interpretation of a large survey) to more than a week (for manual processing and interpretation of a small survey to automated processing and interpretation of a huge survey).

References

[1] Adous, M., X. Dérobert, P. Queffelec, V. Baltzart, L. Laguerre and J. Chazelas, 2006, EM characterization of bituminous concretes over a large frequency bandwidth: First results, In Proceedings of the 11th International Conference on GPR, Ohio State University, Columbus, Ohio.

[2] Al-Qadi, L., A. Loulizi, S. Lahouar. 2000, Dielectric characterization of hot-mix asphalt at the smart road using GPR, In Proceedings of the 8th International Conference on GPR, Gold Coast, Australia.

[3] Benedetto, A., 2004, Theoretical approach to electromagnetic monitoring of road pavement, In Proceedings of the 10th International Conference on GPR.

[4] Benedetto, A., F. Benedetto, M.R. de Blasiis and G. Giunta, 2004, Reliability of radar inspection for detection of pavement damages, International Journal of Road Management and Pavement Design, 5, 93-110.

[5] Benedetto, A. and S. Pensa, 2006, Diagnosis of pavement structural damages using GPR, In Proceedings of the 11th International Conference on GPR, Ohio State University, Columbus, Ohio.

[6] Campman, X., G.C. Herman and E. Muyzert, 2006, Suppressing near-receiver scattered waves from seismic land data, geophysics, 71, S121-S128.

[7] Dashevsky,Y.A., O.Y. Dashesvky, M.I. Filkovsky and V.S. Synakh, 2005, Capacitance sounding: A new geophysical method for asphalt pavement quality evaluation, Journal of Applied Geophysics, 57, 95-106.

[8] Eide, E., P.-A. Sandnes, B. Nilsen and S. Tjora, 2005, Airfield runway inspection using 3-dimensional GPR, In proceedings of the third International Workshop on Advanced GPR, Delft, the Netherlands.

[9] Fauchard, C., X. Dérobert and Ph. Côte, 2000, GPR performances on a road test site, In Proceedings of the 8th International Conference on GPR, Gold Coast, Australia.

[10] Fauchard, C., X. Dérobert and Ph. Côte, 2003, GPR performances for thickness calibration on road test sites, NDT&E International, 36, 67-75.

[11] Fernando, E., W. Liu, B. Dietrich, 2000, A computer program for network level determination of pavement layer thicknesses, In Proceedings of the 8th International Conference on GPR, Gold Coast, Australia.

[12] Grivas, D.A. and H. Shin, 2004 Measuring performance of geotextiles in pavement systems using GPR, In Proceedings of the 10th International Conference on GPR, Delft, The Netherlands.

[13] Grote, K., S.Hubbard, J. Harvey and Y. Rubin, 2005, Evaluation of infiltration in layered pavements using surface GPR reflection trechniques, Journal of Applied Geophysics, 57, 129-153.

[14] Huang,C. and Y. Su, 2004, A new GPR calibration method for high accuracy thickness and permittivity measurement of multi-layered pavement, In Proceedings of the 10th International Conference on GPR, Delft, The Netherlands.

[15] Hugenschmidt, J., M. N. Partl and H. de Witte, 1998, GPR inspection of a mountain motorway in Switzerland,*Journal of Applied Geophysics*, Vol. 40, Nos. 1-3, pp. 95-104

[16] Hugenschmidt, J., 2000, Multi-offset analysis for man-made structures, In Proceedings of the 8th International Conference on GPR, Gold Coast, Australia.

[17] Hugenschmidt, J., 2004, Accuracy and reliability of radar results on bridge decks, In Proceedings of the 10th International Conference on GPR, Delft, The Netherlands.

[18] Inagaki, M. and S. Takarabe, 2006, The ambiguities on a vector diagram for drainage pavement inspection by GPR, In Proceedings of the 11th International Conference on GPR, Ohio State University, Columbus, Ohio.

[19] Jung, G., J. Jung, S.-M. Cho, H. Kim, J. Suh and J. Rhee, 2004, Evaluation of road settlements on soft ground from GPR investigations, In Proceedings of the 10th International Conference on GPR, Delft, The Netherlands.

[20] Kao, C., J. Li, Y. Wang, H. Dong and R. Liu, 2006, Measurement of layer thickness and permittivity using a new multi-layer model from GPR data, In Proceedings of the 11th International Conference on GPR, Ohio State University, Columbus, Ohio.

[21] Kong, F.-N., 2000, Choice of antenna type and frequency range for testing concrete structures, 2000, In Proceedings of the 8th International Conference on GPR, Gold Coast, Australia.

[22] Kruk, J. van der, R.Streich and A.G. Green, 2006, Properties of surface waveguides derived from the sperate and joint inversion of dispersive TE and TM GPR data, Geophysics, 71, K19-K29.
[23] Lambot, S., E.C. Slob, I. van den Bosch, B. Stockbroeckx, B. Scheers and M. Vanclooster; 2004, Modeling of ground penetrating radar for accurate characterization of subsurface dielectric properties. IEEE Transactions on Geoscience and Remote Sensing, Vol. 42, No. 11, p. 2555-2568
[24] Lambot, S., L. Weihermüller, J.A. Huisman, H. Vereecken, M. Vanclooster and E.C. Slob, 2006, Analysis of air-launched ground-penetrating radar techniques to measure the soil surface water content, Water Resources Research, in print.
[25] Lehmann, F. and A.G. Green, 1999,semi-automated geo-radar acquisition in three dimensions, Geophysics, Vol. 64, 836-848.
[26] Liu, L. and T. Guo, 2002, Dielectric property of asphalt pavement specimens in dry, water-saturated and frozen conditions, In Proceedings of the 9th International Conference on GPR, Santa Barbara, California.
[27] Lorenzo, H., M.C. Hemandez and V. Cuellar, 2000, In situ radar remote sensing applied to the detection of degradation in a concrete floor, In Proceedings of the 8th International Conference on GPR, Gold Coast, Australia.
[28] Lualdi, M., L. Zanzi amd G. Sosio, 2006, A 3D GPR survey methodology for archaeological applications, In Proceedings of the 11th International Conference on GPR, Columbus Ohio, USA.
[29] Manacorda, G. and M. Miniati, 2000, An easy way of checking impulsive georadar equipment performances, In Proceedings of the 8th International Conference on GPR, Gold Coast, Australia.
[30] Mesher, D. E. , C. B. Dawley, J.L. Davis and J.R. Rossiter, 1995, Evaluation of new ground-penetrating radar technology to quantify pavement structures, Transportation Research Record 1505, Transportation Research Board, USA, pp. 17-26.
[31] Millard, S.G., J. David, Y.Huang and J.H. Bungey, 2002, A wide band system for measureing dielectric properties of concrete, In Proceedings of the 9th International Conference on GPR, Santa Barbara, California.
[32] Olhoeft, G.R., S.S. Smith III, 2000, Automatic processing and modeling of GPR data for pavement thickness and properties, In Proceedings of the 8th International Conference on GPR, Gold Coast, Australia.
[33] Palli,A., S. Aho and E. Pesonen, 2005, Ground penetrating radar as a quality assurance method for paved gravel roads in Finland, In proceedings of the third International Workshop on Advanced GPR, IWAGPR05, Delft the Netherlands.
[34] Riyanti, C.D., and G.C.Herman, 2005, Three dimensional elastic scattering by near-surface heterogeneities: Geophysical Journal International, 160, 609–620
[35] Roddis, W.M., K. Maser and A. Gisi, 1992, Radar pavement thickness evaluations for varying base conditions, Transportation Research Record 1355, Transportation Research Board, USA, p. 90-98.
[36] Saarenketo, T., and H. Vesa, 2000, The use of GPR technique in surveying gravel road wearing course, In Proceedings of the 8th International Conference on GPR, Gold Coast, Australia.
[37] Slob, E.C., J. van der Kruk and J.T. Fokkema, 2001. GPR Study for Highway Reconstruction in the Netherlands Proceedings of the 63rd EAGE Conference & Exhibition, Amsterdam.
[38] Slob, E.C., J. Groenenboom and J.T. Fokkema, 2003, Automated acquisition and processing of 3D GPR data for object detection and characterization, Subsurface Sensing Technologies and Applications, Vol. 4, 5-18.
[39] Spagnolini, U., 1997, Permittivity measurements of multilayered media with monostatic pulse radar, IEEE Trans. Geosc. & Remote Sens., 35, 454-463.
[40] http://www.allied-associates.co.uk
[41] http://www.aperio.co.uk
[42] http://www.ta-survey.nl
[43] http://www.sensoft.ca
[44] http://www.geophysical.com
[45] http://www.idscompany.it
[46] http://www.3d-radar.com
[47] http://www.malags.se
[48] http://www.roadscanners.com
[49] http://www.radsys.lv